Journal of Fluorescence, Vol. 1, No. 2, 1991

Rotational Brownian Dynamics of Semiflexible Broken Rods

Angel Iniesta,[1] M. Carmen López,[1] and José García de la Torre[1,2]

Received March 12, 1991; revised June 26, 1991; accepted June 28, 1991

Using the Brownian dynamics simulation technique, we study the rotational dynamics of a semiflexible broken rod. We employ a suitable bead model with stiff springs between beads and strong forces opposing to bending, except at the joint where flexibility is variable. We consider mostly broken rods with equal arms. From the simulated Brownian trajectories we obtain the correlation function for the second order Legendre polynomial of the reorientational angle of the end-to-end vector and of the arm vector. These correlation functions are closely related to fluorescence anisotropy decay and electric birefringence decay, respectively. In the first case, the relaxation time for a completely flexible rod agrees with the Harvey–Wegener theory, and in the second, the longest relaxation time agrees well with that obtained from the rigid-body treatment over the whole range of flexibility. Furthermore, we discuss the relative importance of flexibility in both types of decay. Finally, we present results for a case with unequal arms, confirming the validity of the Harvey–Wegener theory and the rigid-body treatment.

KEY WORDS: Broken rod; flexibility; anisotropy decay; Brownian dynamics.

INTRODUCTION

Segmentally flexible macromolecules [1] have a few domains or subunits of comparable size joined by more or less rigid connectors. One of the simplest and most important cases is that of some biopolymers, of which the myosin rod [2] is a typical example, having two rodlike subunits joined by a semiflexible joint. The proper model for such cases is the broken rod, which was first studied over 20 years ago [3]. Some works have focused on the calculation of overall hydrodynamic properties such as the sedimentation coefficient and the intrinsic viscosity, which can be conveniently obtained averaging conformationally values calculated for rigidly bent rods [4,5] in terms of the so-called rigid-body treatment [3,6,7]. We have recently presented a comprehensive study of this procedure [8].

A different approach to the dynamics of segmentally flexible macromolecules consists of extending the theory for rigid macromolecules [4,9,10] as to include additional degrees of freedom corresponding to the internal (essentially bending) motions [2,11–16]. In this theory, first proposed by Harvey and Wegener and further developed by other workers, the inversion of a generalized friction matrix gives a generalized diffusion matrix from which diffusion coefficients corresponding to various reorientational modes can be obtained. The theory is restricted to the case of total flexibility at the hinges.

As both approaches suffer some deficiencies in the description of the rotational dynamics of the whole molecule or that of its parts, we recently undertook [17] the simulation of the Brownian dynamics [18,19] of a simplistic model with three beads, the elastic trumbbell [20–22]. Comparing results from both formalisms with the simulated ones, we were able to find out that the rigid-

[1] Departamento de Química Física, Facultad de Ciencias Químicas, Universidad de Murcia, 30100-Murcia, Spain.
[2] To whom correspondence should be addressed.

1053-0509/91/0600-0129$06.50/0

body treatment is quite accurate in the prediction of the reorientational rate for the end-to-end vector over the whole range of flexibility, while the reorientation of the individual subunits had a different rate that agreed well for the flexible case with the Harvey–Wegener (HW) theory [2,11] including hydrodynamic interaction [12,14].

We now present a Brownian dynamics simulation of a broken rod with a semiflexible swivel-like joint. We have used several values for the flexibility parameter of the joint, obtaining, from simulated trajectories, correlation functions related to the decay of different time-dependent electrooptical properties. Thus, we can find rotational relaxation times observed in fluorescence anisotropy decay [2,11], τ_i ($i = 1,2$) and the one corresponding to the decay of the electric birefringence [21,23,24], τ_a. In all the cases the data obtained with the Brownian simulation technique have been compared with the rigid treatment results [8] (τ_a) or with the results of Wegener [11] (τ_i).

METHODS

The broken rod is modeled, as shown in Fig. 1, using $N = 1 + n_1 + n_2$ touching beads with diameter b. n_1 and n_2 are, respectively, the beads in each arm, and an additional bead represents the hinge. Actually, adjacent beads are held together by a stiff spring with equilibrium length b and a potential quadratic in the displacement with respect to b, with a spring constant such that the fluctuation in bond length is only 10%. Previous calculations for related models [17,25] have shown that these choices results in a good representation of a rigid bond. Thus, the length of the molecule can be taken as $L = Nb$. Due to the slowness of Brownian dynamics simulation with hydrodynamic interaction (computer time proportional to N^3), we have taken just $N = 11$. From previous works [4,8,26,27] it is expected that, if properties are properly scaled to L, the results will be quite insensitive to the choice of N since it usually influences the dynamics in the form of $\ln N$. In most of the calculation we considered arms of equal length since in that way the difference between the broken rod and the straight one is greatest. In some cases, we considered different arm lengths to observe their different mobility.

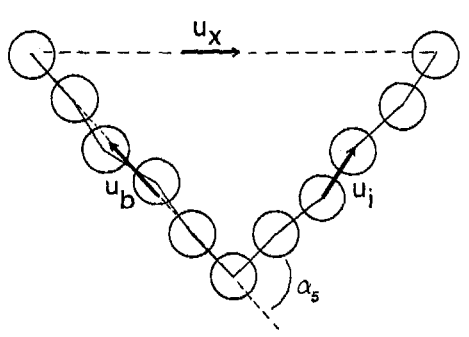

Fig. 1. Geometry of the semiflexible broken rod with $N = 11$ ($n_1 = n_2 = 5$) in an instantaneous conformation determined by the central angle, α_5. The unitary vectors describing the orientations of the bonds (u_i), arms (u_b), and end-to-end vector (u_x) are shown.

We denote as $\mathbf{b}_i$ the bond vector going from the center of bead i to that of bead $i + 1$. α_i is the angle subtended by vectors $\mathbf{b}_{i-1}$ and $\mathbf{b}_i$ (determined by beads $i = i - 1$, i, and $i + 1$). We assume a bending potential normalized to thermal energy kT, which is also quadratic in the displacement with respect to an equilibrium value supposed to be zero (beads aligned) and with a stiffness parameter Q. Thus,

$$V_{b,i} = Q\alpha_i^2 \tag{1}$$

If beads $i - 1$, i, and $i + 1$ are in the same arm (including the case in which either bead $i - 1$ or bead $i + 1$ is the hinge), we take a supposedly very high value for the parameter, $Q_\infty = 50$ (under Results section we just say $Q \to \infty$), so that the beads will be practically collinear. The fluctuation $\langle \Delta\alpha^2 \rangle^{1/2}$ is only 0.16 radian. In other words, the arms are like very stiff worm-like chains with a ratio of persistence to total length equal to 0.965, which corresponds to a practically rod-like behavior.

On the other hand, if bead i is at the joint, we take varying values for Q, between 0 and 50 (practically ∞), so that this parameter determines the flexibility of the hinged rod and will be essential in the calculations and the Discussion.

In the Appendix we give more details about the mechanical properties of the model and present explicit expressions for the forces.

The numerical work was performed in reduced form, as described elsewhere[25]. The unit in which we express translational diffusion is $k_BT/6\pi\eta_0(b/2)$, where k_BT, is the Boltzman exponential, η_0 the solvent viscosity, and b the diameter of the subunits. Rotational diffusion is in units of $k_BT/6\pi\eta_0(b/2)^3$ and the reciprocal of the latter is the unit of time.

The computer requirements of Brownian dynamics simulation with hydrodynamic interaction made it necessary to optimize the simulation conditions with regard to both procedure and working parameters. In the first aspect, the use of a second-order algorithm that we have recently studied [28], instead of the first-order, Ermak–McCammon [18] procedure, was crucial to speed up the

simulation. With regard to working conditions the time step was $\Delta t = 0.0005$ in the dimensionless form. The Brownian trajectory was arbitrarily started from a straight conformation of the rod (which is indeed the conformation of minimum energy). Anyhow, the results are independent of this choice, since the memory of the initial conformation is lost after a moderate number of steps.

The total number of steps was $5 \cdot 10^5$, so the length of the trajectory was 250. The conformation of the model was recorded every five steps, so that a set of 100,000 data was available for the correlation analysis. We have verified that this is the optimum value, because a shorter trajectory is not sufficient to show the internal and overall motions, and on the other hand, with larger trajectories important accumulative errors that effect the precision of the data have been observed. In all the cases the trajectory was divided into five subtrajectories (five subsets of 20,000 conformations) with a length of 50, and the correlation functions were calculated for each of them. For a given value of time, the results of the correlation function for the various subtrajectories were combined, calculating their mean and standard deviation. The former is taken as the final value of the correlation function, and the latter is used to estimate the statistical error of the procedure which is indicated by means of the error bars in the following figures. Hydrodynamic interaction was included rigorously in all our simulations, using Yamakawa–Rotne–Prager tensors [9].

RESULTS AND DISCUSSION

We first analyzed the time correlation function $\langle P_2 \rangle \equiv \langle P_2(\cos\theta_x) \rangle$, where θ_x is the angle subtended by two orientations of the end-to-end vector, separated by time t. The decay of this function is related to the decay of the electric birefringence. Some results are presented in Fig. 2. For all the values of Q the decay is linear in the semilogarithmic plot, so that it can be represented by

$$\langle P_2 \rangle_x \equiv \exp(-t/\tau_a) \qquad (2)$$

where τ_a is the relaxation time for the end-to-end vector. The results are listed in Table I. In the rigid-body treatment for rotational relaxation, $1/\tau_a$ is obtained as a conformational average over rigid-bent-rod values as described in our previous paper [8]. It is evident from the results in Table I that such treatment gives results that are in excellent agreement with the simulation. We remark that, as noted in Ref. 8, the relaxation time increases by a factor $\tau_\alpha(\infty)/\tau_\alpha(0) \cong 2$ on going from the completely flexible to the rigid (straight) rod.

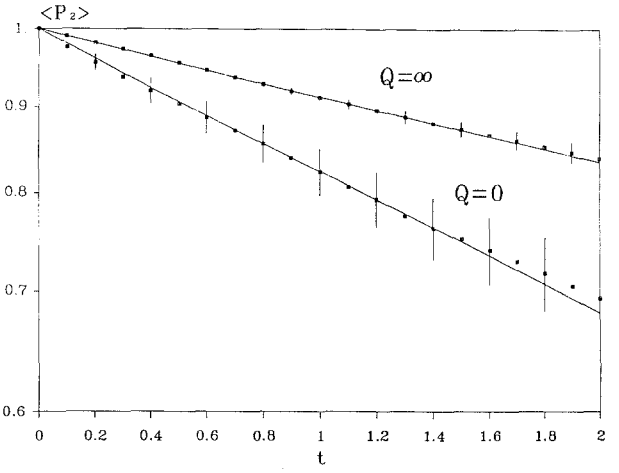

Fig. 2. Plot of the decay of the $\langle P_2 \rangle_x$ function, corresponding to the reorientation of the end-to-end vector, for a rod with equal arms for the two extreme flexibility cases, $Q = 0$ and $Q = \infty$.

Table I. Relaxation Times in Reduced Units for the End-to-End Vector of a Rod of Equal Arms ($n_1 = n_2 = 5$)

	$1/\tau_a$	
Q	RB[a]	DB[b]
0.	0.181	0.190
0.2	0.153	0.141
0.3	0.142	0.132
0.5	0.127	0.121
1.	0.109	0.108
2.	0.098	0.099
∞	0.087	0.089

[a]Rigid-body treatment.
[b]Brownian dynamics simulation.

We next analyzed the time correlation function $\langle P_2 \rangle_b \equiv \langle P_2(\cos\theta_b) \rangle$, where θ_b is the angle subtended by two orientations, separated by time t, of the arm vector, which is a unitary vector in the direction that goes from the joint to the end of the arm. This function corresponds now to the rotation of one arm more or less independently of the other (depending on the flexibility of the joint) and it is closely related to the decay of fluorescence anisotropy; the decays of $\langle P_2 \rangle_b$ and anisotropy are indeed coincident if either the absorption or the emission moments are along the arm. Otherwise the anisotropy decay would have a component associated to torsional rotation of the subunits along their long exes. This component would relax typically much faster than those considered here. As our simulation algorithm cannot deal with such torsional motions, we overlook that possible

component. In fact, we just consider the decay of $\langle P_2 \rangle$, which do not depend on the specific orientations of the emission and absorption moments.

In our preliminary study of the segmentally flexible trumbbell we have shown that the decay of $\langle P_2 \rangle_b$ is different from that of $\langle P_2 \rangle_x$. Indeed, this is evident from the results shown in Fig. 3. Now, a good description of the decay requires a double-exponential fitting function:

$$\langle P_2 \rangle_b = A\exp(-t/\tau_1) + (1-A)\exp(-t/\tau_2) \quad (3)$$

mostly for intermediate Q. The results for τ_1, τ_2, and the amplitude A are listed in Table II.

The second relaxation time τ_2 characterizes the initial depolarization noticed in the period $0 \leq t \leq 0.4$ and has an error larger than that of the first one. This fact, along with the lack of a trend in the data for various Q's, suggests that τ_2 may be independent of the flexibility of the hinge. For intermediate Q's, τ_2 is only twice shorter than τ_1. For very flexible broken rods our results suggest $\tau_2/\tau_1 \cong 1/5$, while for very stiff ones τ_z will be one or more orders of magnitude shorter. Anyhow, this effect may be difficult to verify experimentally, and on the other hand, there is no available theory against which our simulation data could be compared.

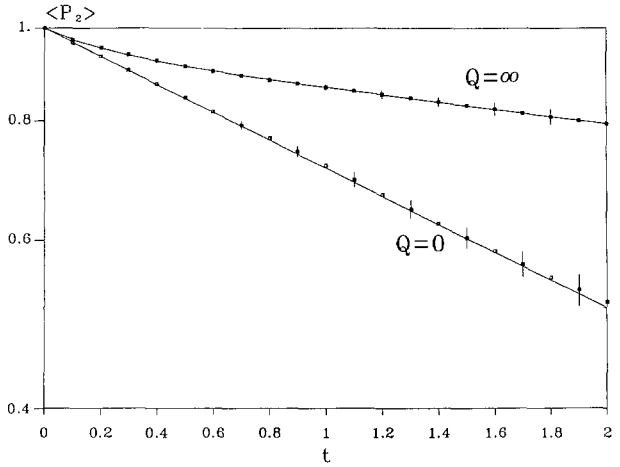

Fig. 3. The same as in Fig. 1 for the function $\langle P_2 \rangle_b$ corresponding to the reorientation of the arms.

Table II. Relaxation Times in Reduced Units for the Arm Vector of a Rod of Equal Arms ($n_1 = n_2 = 5$)

			BD[c]		
Q	$1/\tau_1$ RB[a]	$1/\tau_1$ HW[b]	A	$1/\tau_1$	$1/\tau_2$
0.	—	0.338	0.99	0.35	—
0.2	—	—	0.96	0.32	3.0
0.5	—	—	0.96	0.26	4.2
1.	—	—	0.95	0.24	3.6
2.	—	—	0.90	0.186	2.9
∞	0.087	—	0.93	0.089	4.4
			Average		3.6

[a]Rigid-body treatment.
[b]Harvey–Wegener theory including IH.
[c]Brownian dynamics simulation.

Therefore we concentrate our analysis of $\langle P_2 \rangle_b$ in the long time region (say $t > 0.4$), which is determined by the longest relaxation time, τ_1. We see in Table II how the result for τ_1 from the Harvey–Wegener[2,11] treatment for the completely flexible case including hydrodynamic interaction[15] is in excellent agreement with that from the simulation. Thus, we verify for the hinged rod our conclusion previously obtained with the trumbbell model, about the correctness of the Harvey–Wegener treatment of segmentally flexible macromolecules.

We note that the longest relaxation time for the arm relaxation, τ_1, is more sensitive to flexibility than that for the end-to-end, τ_a. Indeed, we obtain $\tau_1(\infty)/\tau_1(0) \cong 4$. Thus, properties of the type of fluorescence anisotropy decay are more sensitive to flexibility than other properties such as birefringence decay. Furthermore, there is a qualitative aspect that may be even more relevant from the point of view of data interpretion: while the electric birefringence decay is expected to be a single exponential for rigid, semiflexible, and completed flexible rods, in the case of the decay of fluorescence anisotropy or similar properties, a double-exponential behavior could be found for broken rods of intermediate flexibility.

We finally present results for a single case in which the joint is not at the middle of the rod, and the arms are unequal. $\langle P_2 \rangle_x$ was again monoexponential, with relaxation times listed in Table III. $\langle P_2 \rangle_b$ was again fitted to a double-exponential function, but the behavior was practically monoexponential in most cases ($A = 0.92$ or

Table III. Relaxation Times in Reduced Units for a Rod with Unequal Arms $n_1 = 4$, $n_2 = 8$

	$1/\tau_a$		$1/\tau_1$, short arm		$1/\tau_1$, long arm	
Q	RB[a]	BD[b]	BD	HW[c]	BD	HW
0.	0.094	0.096	0.52	0.54	0.133	0.136
0.5	0.075	0.078	0.51	—	0.120	—
∞	0.057	0.057	0.06	—	0.054	—

[a]Rigid-body treatment.
[b]Brownian dynamics simulation.
[c]Harvey–Wegener theory including IH.

0.97 when $Q \to \infty$ and $A \cong 1$ in other cases). Although the break is not at the middle, the ratio $\tau_a(\infty)/\tau_a(0) \cong 2$ still holds. The performance of the rigid-body treatment is again very good. For the relaxation time of the arms, the Harvey–Wegener theory is in good agreement with simulation, as in the previous case.

The variation of the relaxation times τ_1 with Q shows clearly a tendency that could already be perceived for $n_1 = n_2$. We see that for a typically intermediate value $Q = 0.5$ (which is about that corresponding to myosin rod [8]), for which τ_a is roughly halfway between $\tau_a(\infty)$ and $\tau_a(0)$, the value of τ_1 is much closer to $\tau(0)$ than to $\tau(\infty)$. In other words, a much smaller amount of flexibility is required to make an appreciable decrease in the relaxation time (with respect to that of the straight rod) in the case of τ_1 (anisotropy decay) than for τ_a (birefringence decay). A related conclusion is that the HW values, that which are strictly valid only for Q = 0, give reasonable estimates of the arm relaxation of quite stiff rods. Thus, the Harvey–Wegener treatment can be useful in preliminary interpretation of data for semiflexible broken rods, and this is probably the case for other segmentally flexible macromolecules.

APPENDIX

Stretching Forces

The bond between two neighbor beads is regarded as a strong spring with an harmonic potential. For the bond i we have

$$V_{s,i} = \frac{kT}{2\delta^2}(b_i - b_0)^2, \qquad i = 1, \ldots, N-1 \quad \text{(A1)}$$

where b_0 is the equilibrium length, b_i the instantaneous distance between subunit i and subunit $i+1$, and δ is the spring constant. The stretching force acting on subunit i, $\mathbf{F}_{s,i}$, can be obtained from the derivatives of Eq. (A1) with respect to its position vector, $\mathbf{r}_i$. Thus,

$$\mathbf{F}_{s,1} = \mathbf{M}_1 \quad \text{(A2.a)}$$

$$\mathbf{F}_{s,i} = \mathbf{M}_i - \mathbf{M}_{i-1}, \; i = 2, \ldots, N-1 \quad \text{(A2.b)}$$

$$\mathbf{F}_{s,N} = -\mathbf{M}_N \quad \text{(A2.c)}$$

where

$$\mathbf{M}_{s,i} = -kT\frac{1-b_i}{\delta_i^2}\mathbf{u}_i \quad \text{(A3)}$$

and $\mathbf{u}_i = \mathbf{b}_i/b_i \cdot \mathbf{b}_i$ is the unitary bond vector. In Eq. (A3) we have taken $b_0 = 1$.

Bending Forces

With regard to the angles α_i between bonds, the bending potential is considered quadratic in the displacement with respect to the equilibrium value, α_0,

$$V_{B,i} = \frac{1}{2}(\alpha_i - \alpha_0)^2\frac{kT}{\gamma^2}, \quad i = 1, \ldots, N-2 \quad \text{(A4)}$$

where γ is the angular stiffness parameter. From this equation we obtain Eq. (1) considering $Q = \frac{1}{2}\gamma^2$, taking $\alpha_0 = 0$, and normalizing to thermal energy kT.

This potential is a function of the position of the subunits i, $i+1$, and $i+2$. The bending force for each subunit is obtained from the derivatives of terms given by Eq. (A4):

$$\mathbf{F}_{B,1} = \mathbf{A}_{1,1} \quad \text{(A5.a)}$$

$$\mathbf{F}_{B,2} = \mathbf{A}_{1,2} + \mathbf{A}_{2,1} - \mathbf{A}_{1,1} \quad \text{(A5.b)}$$

$$\mathbf{F}_{B,i} = \mathbf{A}_{i-1,2} - \mathbf{A}_{i-2,2} + \mathbf{A}_{i,1} - \mathbf{A}_{i-1,1}, \quad i = 1, \ldots, N-2 \quad \text{(A5.c)}$$

$$\mathbf{F}_{B,N-1} = \mathbf{A}_{N-2,2} - \mathbf{A}_{N-3,2} - \mathbf{A}_{N-2,1} \quad \text{(A5.d)}$$

$$\mathbf{F}_{B,N} = -\mathbf{A}_{N-2,2} \quad \text{(A5.e)}$$

where

$$\mathbf{A}_{i,1} = kT\left[\frac{\alpha_i}{\gamma_i^2 \operatorname{sen}\alpha_i b_i}\right]\cdot(-\mathbf{u}_{i+1} + \cos\alpha_i \mathbf{u}_i) \quad \text{(A6.a)}$$

and

$$\mathbf{A}_{i,2} = kT\left[\frac{\alpha_i}{\gamma_i^2 \operatorname{sen}\alpha_i b_{i+1}}\right]\cdot(-\mathbf{u}_i + \cos\alpha_i \mathbf{u}_{i+1}) \quad \text{(A6.b)}$$

In Eq. (A6) we have taken $\alpha_0 = 0$.

Total Forces

The sum of the stretching contributions and that from bending give the total force at each bead,

$$\mathbf{F}_i = \mathbf{F}_{B,i} + \mathbf{F}_{S,i} \quad \text{(A7)}$$

ACKNOWLEDGMENT

This work was supported by Grant PB87-0694 from Direccion General de Investigacion Cientifica y Tecnica to J.G.T.

REFERENCES

1. J. Yguerabide, H. F. Epstein, and L. Stryer (1970) *J. Mol. Biol.* **51,** 573.
2. S. C. Harvey (1979) Biopolymers **18,** 1081.
3. H. Yu and W. H. Stokmayer (1967) *J. Chem. Phys.* **47,** 1369.
4. J. García de la Torre and V. A. Bloomfield (1978) *Biopolymers* **17,** 1605.
5. W. A. Wegener (1984) *Biopolymers* **23,** 2243.
6. G. Wilemski (1977) *Macromolecules* **10,** 28.
7. J. J. García Molina and J. García de la Torre (1984) *Int. J. Biol. Macromol.* **6,** 170.
8. A. Iniesta, F. G. Díaz, and J. García de la Torre (1988) *Biophys. J.* **54,** 269.
9. J. García de la Torre and V. A. Bloomfield (1981) *Q. Rev. Biophys.* **14,** 81.
10. J. García de la Torre (1989) in S. E. Harding and A. J. Rowe (Eds.), *Dynamic Properties of Biomolecular Assemblies,* Royal Society of Chemistry, Cambridge.
11. W. A. Wegener (1980) *Biopolymers* **19,** 1899.
12. S. C. Harvey, P. Mellado, and J. García de la Torre (1983) *J. Chem. Phys.* **78,** 2081.
13. J. García de la Torre, P. Mellado, and V. Rodes (1985) *Biopolymers* **24,** 2145.
14. W. A. Wegener (1982) *J. Chem. Phys.* **76,** 6425.
15. P. Mellado, A. Iniesta, F. G. Díaz, and J. García de la Torre, (1988) *Biopolymers* **27,** 1771.
16. R. F. Goldstein (1985) *J. Chem. Phys.* **83,** 2390.
17. F. G. Díaz and J. García de la Torre (1988) *J. Chem. Phys.* **88,** 7698.
18. D. L. Ermak and J. A. McCammon (1979) *J. Chem. Phys.* **69,** 1352.
19. S. A. Allison and J. A. McCammon (1984) *Biopolymers* **23,** 167.
20. O. Hassager *J. Chem. Phys. (1974)* **60,** 2111.
21. K. Nagasaka and H. Yamakawa (1985) *J. Chem. Phys.* **83,** 6480.
22. D. Roitman and B. H. Zimm, *J. Chem. Phys.* (1984) **81,** 6348.
23. D. Roitman and B. H. Zimm, *J. Chem. Phys.* (1984) **81,** 6348.
24. D. Roitman (1984) *J. Chem. Phys.* **81,** 6356.
25. F. G. Díaz, A. Iniesta, and J. García de la Torre (1987) *J. Chem. Phys.* **87,** 6021.
26. P. Mellado and J. García de la Torre (1982) *Biopolymers* **21,** 1857.
27. S. A. Allison (1986) *Macromolecules* **19,** 118.
28. A. Iniesta and J. García de la Torre (1990) *J. Chem. Phys.* **92,** 2015.